ACS APPLIED MATERIALS & INTERFACES

Research Article

www.acsami.org

Improving Hematite-based Photoelectrochemical Water Splitting with Ultrathin TiO_2 by Atomic Layer Deposition

Xiaogang Yang,*[,†,‡,⊥] Rui Liu,[‡,⊥] Chun Du,[‡] Pengcheng Dai,[‡,§] Zhi Zheng,[†] and Dunwei Wang[‡]

[†]Key Laboratory of Micro-Nano Materials for Energy Storage and Conversion of Henan Province, Institute of Surface Micro and Nano Materials, Xuchang University, Xuchang, Henan 461000, People's Republic of China

[‡]Department of Chemistry, Merkert Chemistry Center, Boston College, 2609 Beacon Street, Chestnut Hill, Massachusetts 02467, United States

[§]Department of Chemistry, Shandong University, Jinan, Shandong 250100, People's Republic of China

Supporting Information

ABSTRACT: Ultrathin TiO_2 was grown on hematite surface by atomic layer deposition (ALD). Obvious photoelectrochemical water oxidation performance improvement was observed for samples treated with as few as a single cycle of TiO_2 deposition. Up to 100 mV cathodic shift of the turn on potential was measured on samples treated by 20-cycle ALD TiO_2. Photocurrent improvement was also measured on samples treated by ALD TiO_2. Systematic studies ruled out possibilities that the improvement was due to electrocatalytic or bulk doping effects. It was shown that the surface treatment led to better charge separation, less surface charge recombination and, hence, greater photovoltage by hematite. The facile surface treatment by ultrathin TiO_2 may find broad applications in the development of stable and high-performance photoelectrodes.

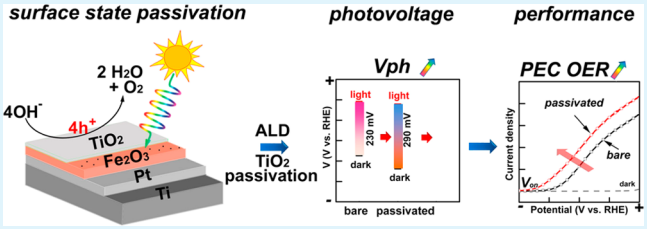

KEYWORDS: *solar water splitting, hematite, TiO_2, photovoltage, photoelectrochemistry, passivation*

INTRODUCTION

Rapid increase of global energy needs and the negative environmental impact by the usage of fossil fuels have made the utilization of clean, renewable energy sources such as solar energy an urgent task.[1] A key challenge in solar energy harvesting is the intermittent nature of sunlight, which necessitates a large-scale energy storage solution.[2] Photoelectrochemical (PEC) water splitting holds the potential to meet the challenge because it can directly store the harvested solar energy in chemical bonds of energetic chemicals such as hydrogen.[2−4] Although a topic of intense research for over 40 years, PEC water splitting progresses at a slow pace. The key issue has been the lack of photoelectrode materials, in particular, those for water oxidation, which can offer high efficiency at a low cost.[5]

Among various candidates studied, hematite (α-Fe_2O_3) represents a protypical material that deserves special attention. On the one hand, it is an earth abundant compound with a medium band gap (2.0−2.2 eV) that can enable solar-to-hydrogen (STH) conversion efficiencies up to 15.3%.[6] In addition, hematite is stable against photocorrosion in alkaline solutions.[6,7] On the other hand, most problems found in other metal oxide semiconductors including short minority charge diffusion distance, low optical extinction coefficient in the visible range and poor water oxidation kinetics are all present in hematite.[8,9] The promise it holds and the challenges it presents make hematite a desired study platform to understand materials for PEC water splitting. Indeed, many strategies designed to improve the photoelectrodes for better PEC water splitting have been tested on hematite. For instance, nanostructuring has been shown to improve charge transport in hematite;[10−12] light absorption could be increased by adding components for multireflections;[13] the carrier concentration may be boosted by introducing dopants;[14,15] the onset potentials (V_{on}, the lowest potential at which photocurrents are measured) are decreased by changing the band edge positions,[16] passivating the surface states[17,18] or applying catalysts.[7,19,20] These intense efforts notwithstanding, the energy convesion efficiencies of hematite are still significantly lower than the theoretical value.[6] The lack of a detailed understanding on the semiconductor/water interface is an important reason why research has progressed slowly.

Consider treatments aimed at reducing V_{on} as an example. Factors that can contribute to reducing V_{on} include the increase of photovoltage (V_{ph}) and the reduction of kinetic overpotential, both highly sensitive to the nature of the hematite/water interface. When a lower V_{on} is observed, knowing which factor plays a more important role is critical because the knowledge helps guide future research to further improve the peformance.[21] In an effort to distinguish these factors, we have

Received: February 13, 2014
Accepted: July 28, 2014
Published: July 28, 2014

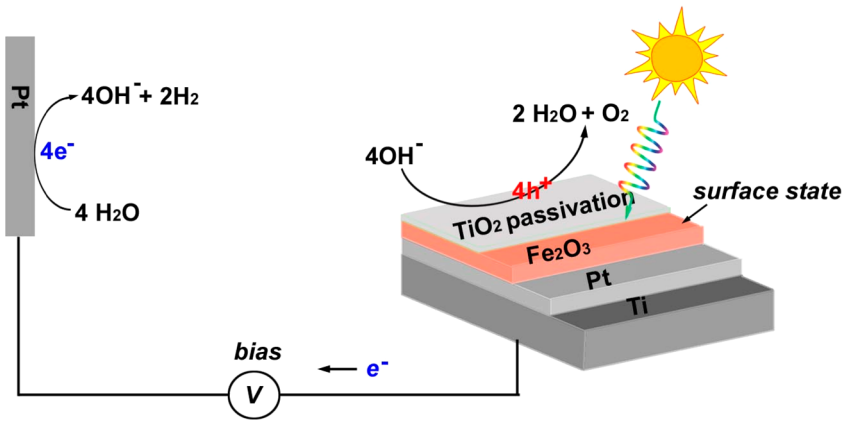

Figure 1. Schematic drawing of the test cell configuration of TiO_2-passivated hematite for water splitting. For clarity, the reference electrode is not shown.

recently examined two water oxidation catalysts, MnO_x and $NiFeO_x$, respectively, and obseved how they changed the performance of hematite.[20,22] Although the effects were in stark contrast, with MnO_x producing drastically higher and $NiFeO_x$ yielding dramatically lower V_{on}'s, changes in V_{ph} were the key reason for the observed differences in both cases. Here we extend our study to ultrathin TiO_2 and show that a coating as thin as 0.8 nm is sufficient to reduce V_{on} by >100 mV. Different from previous reports by Grimes[23] and others,[24,25] our present work demonstrates a surface passivation effect by TiO_2, resulting in increased photovoltage and better PEC water oxidation performance.

EXPERIMENTAL SECTION

Synthesis of Hematite Films. Ti foil (Sigma, 0.127 mm, 99.7%) was cleaned sequentially with acetone, methanol and 2-propanol, and blown dry using N_2. For good conductivity and stability during the thermal annealing of hematite at higher temperature, a layer of 100 nm Pt coating was deposited on the Ti foil with an e-beam thermal evaporator (Sharon Vacuum), before atomic layer deposition (ALD) growth. Iron *tert*-butoxide (prepared as reported), Ti(*i*-PrO)$_4$ and deionized water (18 MΩ) were used as ALD precursors. NaOH (Alpha, 97%; 1.0 M concentration) solution was used as the electrolyte for PEC measurements.

Fe_2O_3 films: detailed information about the synthesis of Fe_2O_3 by atomic layer deposition (ALD: Savannah system, Cambridge Nanotech) at 180 °C has been reported previously.[12] Briefly, the growth was carried out for 400 cycles (estimated thickness: 25 nm). The Fe precursor was maintained at 117 °C to yield appreciable vapor pressure, and H_2O was used at room temperature. After growth, the film was annealed at 500 °C for 20 min in ambient air.

TiO_2 layer: the TiO_2 was deposited on annealed hematite or conductive substrate (Pt-coated Ti foil) by ALD (Savannah system, Cambridge Nanotech) following parameters reported previously.[26] The growth was carried out at 275 °C with Ti(*i*-PrO)$_4$ (maintained at 75 °C) and H_2O (room temperature) as Ti and O precursors, respectively. Before each deposition, the bubbler of the Ti precursor was purged to remove the excess pressure to avoid uncharacteristically fast deposition during the first cycle. The deposition rate was estimated to be 0.04 nm/cycle. After growth, the films were annealed at varying temperatures for 0.5 h in air.

Material Characterization. After preparation, bare hematite and those with TiO_2 decorations were fashioned into electrodes as we have published previously,[22] with an electrical wire connected on the back side by conductive epoxy and sealed in nonconductive epoxy resin. To study the Tafel behavior of TiO_2, Pt-coated Ti foil was used as a substrate onto which the TiO_2 sample was grown. PEC measurements were conducted on a CHI 609 potentiostat (CH Instrument) in a three-electrode configuration, with Fe_2O_3 (with or without TiO_2 decoration) as the working electrode, a Pt wire as the counter electrode and a Hg/HgO in 1.0 M NaOH as the reference electrode. The electrolyte was 1.0 M NaOH solution (pH = 13.5) saturated with O_2. The light source was a solar simulator (Oriel, model 96000) equipped with a AM 1.5 filter with the illumination intensity calibrated to 100 mW/cm^2 by a thermopile optical detector (Newport, Model 818P-010-12).

Electrochemical Tests. All potentials reported here were normalized to reversible hydrogen potential (RHE) unless specified. Current density−voltage (J−V) plots of bare Fe_2O_3 and Fe_2O_3/TiO_2 photoelectrodes were generated under light and dark conditions in 1.0 M NaOH, with a scanning rate of 20 mV/s between 0.8 and 1.6 V. Electrochemical impedance spectroscopy (EIS) was collected in 1.0 M NaOH solution, with an amplitude of 5 mV and frequencies varying between 1 and 100 000 Hz within a potential window of 0.7−1.7 V. Photovoltage measurements were carried out following an open circuit potential method using a three-electrode configuration under dark and light conditions as reported by us previously.[20,22]

RESULTS AND DISCUSSION

Hematite was grown on Pt-coated Ti foil by atomic layer deposition (ALD) and annealed in air following previously published protocols (see the Experimental Section). Although the Pt-coated Ti foil is different from the common fluorine-doped tin oxide (FTO) substrates, and the back reflection of the Pt substrate would increase the light absorption,[13] the comparison between the bare and TiO_2-modified hematite is based on the same substrate and can be applied for the evaluation of the surface TiO_2 modification. After ALD growth of ultrathin TiO_2, the hematite substrate was subjected to annealing in ambient air at 500 °C for 30 min before it was fashioned into a photoelectrode. As schematically shown in Figure 1, all photoelectrochemical and electrochemical data presented in this paper were collected in a three-electrode configuration, where hematite was the working electrode, a Pt wire was the counter electrode and a Hg/HgO electrode (in 1 M NaOH) was the reference electrode.

It has been established by our previous research that the average growth rate of TiO_2 by ALD was 0.4 Å /cycle.[26] The nominal thickness of TiO_2 by 1, 20 and 50 cycles of ALD was estimated as 0.04, 0.8 and 2 nm, respectively. Films thinner than 1 nm are not expected to make a continuous coverage. Yet, the effect on the PEC performance was clear, as shown in Figure 2, with up to 100 mV cathodic shift in V_{on}. If we define V_{on} as the potential at which 0.02 mA/cm^2 current density is first measured,[18] V_{on}'s for hematite treated with 0.04, 0.8 and 2

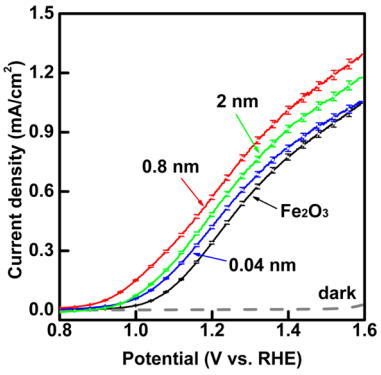

Figure 2. *J*–*V* plots of hematite with and without TiO_2 decorations in 1.0 M NaOH aqueous electrolyte (scan rate 20 mV/s) under simulated solar illumination (AM 1.5, 100 mW/cm^2). For comparison, the polarization curve of bare hematite without illumination is included (labeled as dark).

nm TiO_2 are 0.92, 0.88 and 0.94 V, respectively, showing obvious cathodic shift compared with 1.00 V for bare hematite. To confirm that the observed cathodic shift is not merely a result of a postgrowth annealing effect, we characterized hematite photoelectrodes subjected to identical annealing treatments but without TiO_2 overlayer. No measurable cathodic shift was observed. In addition, the ultrathin TiO_2 decoration also increased the photocurrent densities to 0.821, 1.014 and 0.918 mA/cm^2 at 1.4 V (vs RHE), respectively, corresponding to 6%, 31% and 18% improvement compared to 0.775 mA/cm^2 of bare hematite at the same potential. (Notice: 1% improvement was obtained at 1.6 V vs RHE by one single ALD layer treatment, which is lower than the average error of 2% and should not be overinterpreted in Figure S1 and Table S1 (Supporting Information). Careful and systematic analysis of the result is highly suggested before drawing a conclusion.[27,28]) The observed difference, as small as 1%, has been consistently measured on five batches of difference samples, showing that the performance improvement by TiO_2 modification is highly reproducible. The improvement by ultrathin TiO_2 decoration was also confirmed by incident-photon-to-charge efficiency (IPCE) measurements on 0.8 nm TiO_2-decorated hematite and bare hematite photoelectrodes (Figure 3). It was observed that the IPCE was enhanced in the short wavelength range between 280 to 480 nm for the TiO_2-decorated sample, which is possibly due to the holes generated from two difference optical

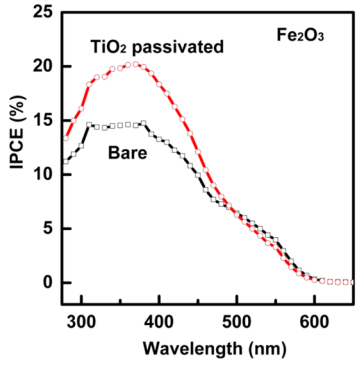

Figure 3. IPCE for TiO_2 (0.8 nm) decorated hematite and bare hematite sample measured under 1.23 V vs RHE in 1.0 M NaOH aqueous electrolyte.

bands of hematite reported by Cherepy et al.[29] and Braun et al.,[30] respectively. The peak value of IPCE on a TiO_2-decorated sample can be as high as 20.1% at 370 nm, whereas only 14.6% was measured on bare hematite at the same wavelength. It is worth noting that the TiO_2-passivated hematite exhibited IPCE enhancements between 400 and 480 nm, whereas the IPCE of TiO_2 photoanode drops close to zero above 380 nm.[26] The result supports that the increased photocurrent is not due to photoresponse of TiO_2. Absorbed-photon-to-charge conversion efficiency (APCE) measurements shown in Figure S2 (Supporting Information) suggest that the photocurrent increase is not a result of better light absorption either.

The existence of Ti on the surface of hematite was confirmed by X-ray photoelectron spectroscopy (XPS, Figure S3 in the Supporting Information). The binding energies of the Ti were 458.5 and 464.3 eV for Ti $2p_{1/2}$ and Ti $2p_{3/2}$, respectively, close to the values for Ti^{4+} rather than Ti^{3+}.[31] TiO_2 control samples of the same growth condition but without hematite were investigated electrochemically, and the results allowed us to rule out the possibility that the increased current is a simple superimposition of TiO_2 and hematite (Figure S4 in the Supporting Information).

The PEC performance increase by TiO_2-decorated hematite may be ascribed to the following reasons: (1) increased light absorption from TiO_2, (2) catalytic properties of TiO_2 that facilitate charge transfer, (3) surface doping effect of Ti and (4) increased minority carrier density in the body of hematite. As discussed above, optical absorption experiments and APCE measurements help rule out the possibility that better light absorption due to TiO_2 decoration was the reason for the improved performance (Figure S2 in the Supporting Information). Next, we use electrochemical impedance spectroscopy (EIS) to quantitatively study charge transfer characteristics of hematite with and without TiO_2 coating.

The impedance data are presented in the form of Nyquist plots in Figure 4. For the measurements in the dark, 1.7 V was chosen because the depletion region of hematite is well developed at this potential. With illumination, an applied potential of 1.1 V was sufficient to drive charge separation, where photocurrents of 0.19 and 0.34 mA/cm^2 were measured for bare and TiO_2-modified hematite samples, respectively. It can be seen from Figure 4 that the impedance changes due to the introduction of the ultrathin TiO_2 layer are insignificant and would not be sufficient to account for the PEC performance difference observed in Figure 2. Upon fitting with equivalent circuit as shown in Figure S5 (Supporting Information),[12,22] the results (in Tables S2 and S3, Supporting Information) showed that the charge transfer resistance (R_{DL}) increased 2.7–3.2 times with the addition of TiO_2 surface decoration in dark conditions; changes in R_{DL} under illumination were insignificant. We also note that the surface state capacitance (C_{SS}) decreased to 20% and 45% under dark and illumination conditions, respectively, when TiO_2 decoration was present. (We also noticed that there are some other kind of equivalent circuits could be used for the simulation of the hematite photoanode.[32]) The result is different from the significant reduction of the charge transfer resistance when a Co–Pi or Co_3O_4 catalyst is applied on hematite.[32,33] This suggests that the TiO_2 layer does not function as an electrocatalyst.

To further support this understanding, we obtained the Tafel plots of bare hematite, hematite decorated by ultrathin TiO_2 and TiO_2 itself in the linear region of 10^{-3}–10^{-1} mA/cm^2. A Tafel plot is popularly used to represent kinetic behaviors of the

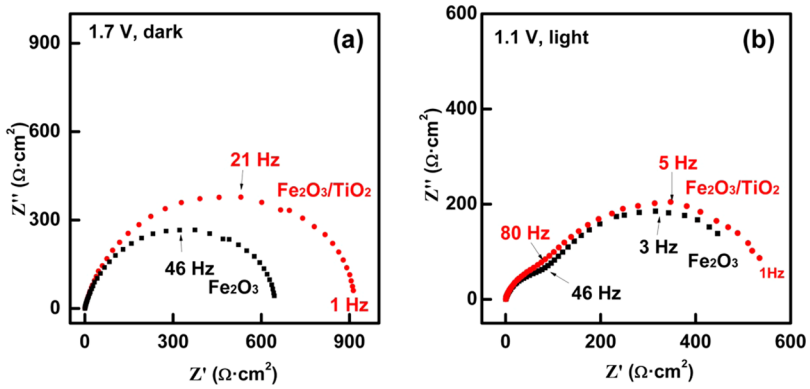

Figure 4. Nyquist plots of bare and TiO_2 (0.8 nm) passivated hematite photoelectrodes measured under different conditions: (a) at 1.7 V in dark; (b) at 1.1 V in light.

more general Butler–Volmer relationship that describes current–voltage characteristics of electrodes.[34] Under ideal conditions, a photoelectrode may be modeled as a photovoltaic coupled with an electrocatalyst, which is analogous to a metallic electrode, when the surface reaction is the rate-limiting step. In the studied potential range (1.5–1.7 V vs RHE), these photoanodes are reasonably conductive, allowing us to study the kinetic behavior on the hematite electrodes in a qualitative manner. As can be seen in Figure 5, all samples exhibited

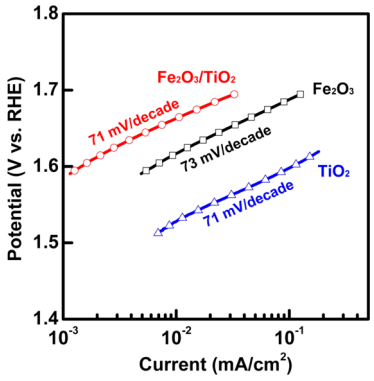

Figure 5. Tafel plots for TiO_2, bare and TiO_2 (0.8 nm) decorated hematite electrodes in 1.0 M NaOH aqueous electrolyte under dark conditions.

comparable slopes of 71 mV/decade, 73 mV/decade and 71 mV/decade, respectively, indicating that there is no obvious change of surface reaction kinetics after TiO_2 treatment. It is noted that all data in Figure 5 were measured in the dark. The current densities of TiO_2 were higher than those of electrodes consisting of Fe_2O_3, presumably because a thicker hematite would require greater bias due to its greater electrical resistance. The Tafel slopes reported here are consistent with a two-dimensional Fe_2O_3 photoanode (74.9 mV/decade),[35] slightly higher than 50–60 mV/decade on ultrathin TiO_2 films reported by Scheuermann et al.[36] The data also agree with the Tafel behavior expected for oxygen evolution reaction when the rate limiting chemical step is a reversible one-electron transfer process.[37] Although the actual oxygen evolution reaction on the electrodes is more complex due to the four electron transfer nature of the reaction, the general Tafel slope of ca. 40 mV/decade is expected for the rate-determining step of oxidation of an OH surface species in the low overpotential region.[38,39] The discrepancy of our measured slopes, as well those in the above-cited reports, may be caused by a number of reasons. For instance, the assumption of a symmetric transfer coefficient of 0.5 may not be valid;[40] the surface roughness was not taken in account; the film thickness may have played a role, too. The data nonetheless highlight that ultrathin TiO_2 does not function as an electrocatalyst.

The possibility that Ti^{4+} may dope the surface of hematite is considered next. It is indeed an important concern because Ti has been reported as an effective doping species that helps improve the performance of hematite by increasing the carrier concentration.[25,41,42] The doping effect, however, is expected to be a function of temperature, as a greater Ti incorporation would result from higher annealing temperatures. Although the performance of TiO_2-decorated hematite was found to indeed increase when the annealing temperature increased from 400 to 500 °C, it decreased when the annealing temperature was further increased to 600 °C (see Figure S5, Supporting Information). The trend is in contrast to the report by Franking et al., in which hematite nanowires were treated by drop-casted $Ti(OBu)_4$.[25] In that report, the authors found that the annealing temperature of 650–700 °C gave rise to the highest photoactivity. Additionally, the increased charge transfer resistance R_{DL} (Table S2, Supporting Information) and the negative V_{on} shift of the TiO_2 treated hematite before annealing (blue curve in Figure S5, Supporting Information) indicated that the surface doping effect should not be the main reason for this improvement. Nevertheless, extensive research is needed to further rule out potential doping effect exerted by the TiO_2 capping layer.

We therefore hypothesize that the performance improvement as shown in Figure 2 is a result of surface photovoltage increase. In other words, the TiO_2 decoration layer acts as a passivation layer to change the hematite–electrolyte interface for a lesser degree of surface recombination and a greater degree of band bending within hematite. The net effect is greater photovoltage, which could be measured by probing the photovoltage under open-circuit conditions.[20,22] As shown in Figure 6, bare hematite exhibited equilibrium potentials of 0.85 V in the dark and 0.62 V under illumination, respectively, corresponding to a 0.23 V photovoltage. The addition of TiO_2 (0.8 nm) increased the equilibrium potential in the dark to 0.92 V and maintained the illuminated open-circuit potential of 0.63 V, yielding a 0.29 V photovoltage. The difference is quantitatively consistent with that observed in Figure 2. In addition, the control electrode with ultrathin TiO_2 layer exhibited a negligible photovoltage of 5 mV, further confirming that the

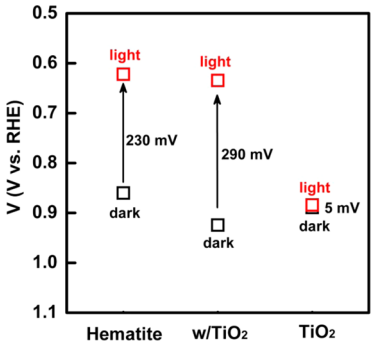

Figure 6. Photovoltage response of hematite photoelectrodes with and without 0.8 nm TiO_2 modification. The bare TiO_2 on substrate is shown as a control photoelectrode.

improvement was not a simple combination of hematite and TiO_2.

To support the hypothesis of the photovoltage increase by surface state passivation effect, transient photocurrent measurement was carried out. In Figure 7, both bare and TiO_2-modified hematite electrodes were studied under a constant bias of 1.1, 1.23 and 1.5 V (vs RHE), respectively. When the light was turned on and off, sharp current spikes were observed, followed by decay to plateau current densities. Compared with data obtained on bare hematite, the integrated area under the current spikes of TiO_2-decorated hematite samples were smaller. The feature is consistent with that obtained on Al_2O_3-passivated hematite.[17] It is important to note that Sivula et al. have previously studied ALD-grown TiO_2 as a surface passivation layer but did not report cathodic shift of the turn-on voltages. We suspect the difference in the growth conditions (200 °C for ref 17 and 275 °C for this work), as well as postgrowth annealing conditions (300 and 400 °C for 20 min for ref 17 and 400–600 °C for 30 min for this work), may be responsible for the device performance differences. Compared with group 13 metal oxides as passivation materials,[17,18] TiO_2 exhibited promising thermodynamic stability under illumination in a wide pH range. Lastly, we note that the PEC performance improvement was also observed in neutral and acidic solutions (Figures S7 and S8, Supporting Information).

CONCLUSION

In conclusion, we successfully passivated a hematite surface with an ultrathin TiO_2 layer by ALD. The TiO_2-passivated photoanodes showed improved photoelectrochemical performance for water oxidation. A layer of coating as thin as 0.04 nm was shown to reduce the negative influence by surface states. The photovoltage measurements support that the performance improvement was due to increased photovoltage generation. However, the surface states on hematite are large even after the surface passivation by TiO_2, showing that more and detailed work is needed for further understanding of the charge recombination behavior at the hematite-electrolyte interface. During the external review of the work, other studies by us and others also showed the significance to reduce/alternate the surface state of hematite, which is regarded as a key challenge during PEC water splitting.[43,44] The treatment of photoelectrodes using ultrathin passivation layers by ALD is expected to find broad applications in the development of stable and high-performing photoelectrode materials for practical solar water splitting.

ASSOCIATED CONTENT

Supporting Information

J–*V* curves, UV–vis absorption and APCE plots, XPS results, EIS simulations and stability of bare Fe_2O_3, TiO_2 and TiO_2-decorated hematite. This material is available free of charge via the Internet at http://pubs.acs.org.

AUTHOR INFORMATION

Corresponding Author

*X. Yang. E-mail: xiaogang.yang@gmail.com.

Author Contributions

⊥These authors contributed equally.

Notes

The authors declare no competing financial interest.

ACKNOWLEDGMENTS

This work was supported by Boston College, NSF (DMR 1055762 and 1317280) and MassCEC. It was also partially supported by Henan Province office of education (14B150013), Innovation Scientists and Technicians Troop Construction Projects of Henan Province (Grant No. 144200510014) and National Natural Science Foundation of

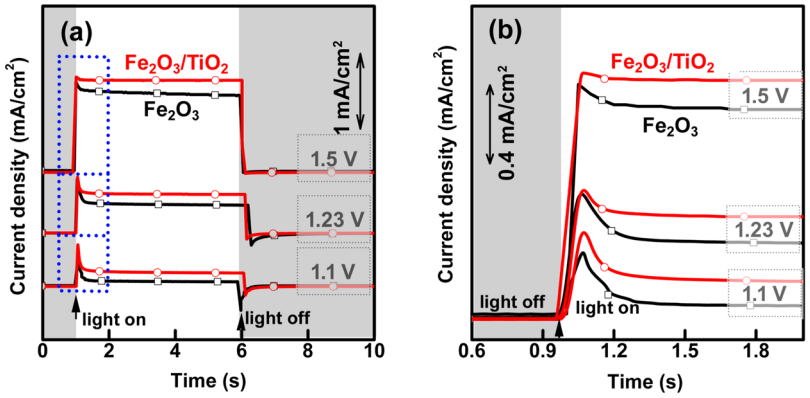

Figure 7. Transient photocurrent response by chopped light as a function of time. Potentials of 1.1, 1.23 and 1.5 V (vs RHE) were applied to bare and TiO_2-passivated hematite: (a) a typical light off (1 s), light on (5 s) and light off (5 s) process; (b) fine feature during the light on in the range from the left figure. The black and red traces correspond to the bare and TiO_2-passivated hematite samples, respectively.

China (No. 21273192). D.W. is an Alfred P. Sloan Fellow. We thank Stephen Shepard at the Boston College Nanofabrication Facilities for his assistance of the metal depositions.

REFERENCES

(1) IEA. *Key World Energy Statistics*; OECD Publishing: Paris, 2010.
(2) Lewis, N. S.; Nocera, D. G. Powering the Planet: Chemical Challenges in Solar Energy Utilization. *Proc. Natl. Acad. Sci. U. S. A* **2006**, *103*, 15729−15735.
(3) Fujishima, A.; Honda, K. Electrochemical Photolysis of Water at a Semiconductor Electrode. *Nature* **1972**, *238*, 37−38.
(4) Walter, M. G.; Warren, E. L.; McKone, J. R.; Boettcher, S. W.; Mi, Q. X.; Santori, E. A.; Lewis, N. S. Solar Water Splitting Cells. *Chem. Rev.* **2010**, *110*, 6446−6473.
(5) Bak, T.; Nowotny, J.; Rekas, M.; Sorrell, C. C. Photo-electrochemical Hydrogen Generation from Water Using Solar Energy. Materials-related Aspects. *Int. J. Hydrogen Energy* **2002**, *27*, 991−1022.
(6) Sivula, K.; Le Formal, F.; Grätzel, M. Solar Water Splitting: Progress Using Hematite (α-Fe_2O_3) Photoelectrodes. *ChemSusChem* **2011**, *4*, 432−449.
(7) Tilley, S. D.; Cornuz, M.; Sivula, K.; Grätzel, M. Light-Induced Water Splitting with Hematite: Improved Nanostructure and Iridium Oxide Catalysis. *Angew. Chem., Int. Ed.* **2010**, *49*, 6405−6408.
(8) Mayer, M. T.; Lin, Y.; Yuan, G.; Wang, D. Forming Heterojunctions at the Nanoscale for Improved Photoelectrochemical Water Splitting by Semiconductor Materials: Case Studies on Hematite. *Acc. Chem. Res.* **2013**, *46*, 1558−1566.
(9) Lin, Y.; Yuan, G.; Sheehan, S.; Zhou, S.; Wang, D. Hematite-based Solar Water Splitting: Challenges and Opportunities. *Energy Environ. Sci.* **2011**, *4*, 4862−4869.
(10) Lindgren, T.; Wang, H. L.; Beermann, N.; Vayssieres, L.; Hagfeldt, A.; Lindquist, S. E. Aqueous Photoelectrochemistry of Hematite Nanorod Array. *Sol. Energy Mater. Sol. Cells* **2002**, *71*, 231−243.
(11) Mohapatra, S. K.; John, S. E.; Banerjee, S.; Misra, M. Water Photooxidation by Smooth and Ultrathin α-Fe_2O_3 Nanotube Arrays. *Chem. Mater.* **2009**, *21*, 3048−3055.
(12) Lin, Y.; Zhou, S.; Sheehan, S. W.; Wang, D. Nanonet-based Hematite Heteronanostructures for Efficient Solar Water Splitting. *J. Am. Chem. Soc.* **2011**, *133*, 2398−2401.
(13) Dotan, H.; Kfir, O.; Sharlin, E.; Blank, O.; Gross, M.; Dumchin, I.; Ankonina, G.; Rothschild, A. Resonant Light Trapping in Ultrathin Films for Water Splitting. *Nat. Mater.* **2013**, *12*, 158−164.
(14) Kay, A.; Cesar, I.; Grätzel, M. New Benchmark for Water Photooxidation by Nanostructured α-Fe_2O_3 Films. *J. Am. Chem. Soc.* **2006**, *128*, 15714−15721.
(15) Zandi, O.; Klahr, B. M.; Hamann, T. W. Highly Photoactive Ti-Doped α-Fe_2O_3 Thin Film Electrodes: Resurrection of The Dead Layer. *Energy Environ. Sci.* **2013**, *6*, 634−642.
(16) Lin, Y.; Xu, Y.; Mayer, M. T.; Simpson, Z. I.; McMahon, G.; Zhou, S.; Wang, D. Growth of p-Type Hematite by Atomic Layer Deposition and Its Utilization for Improved Solar Water Splitting. *J. Am. Chem. Soc.* **2012**, *134*, 5508−5511.
(17) Le Formal, F.; Tetreault, N.; Cornuz, M.; Moehl, T.; Grätzel, M.; Sivula, K. Passivating Surface States on Water Splitting Hematite Photoanodes with Alumina Overlayers. *Chem. Sci.* **2011**, *2*, 737−743.
(18) Hisatomi, T.; Le Formal, F.; Cornuz, M.; Brillet, J.; Tetreault, N.; Sivula, K.; Grätzel, M. Cathodic Shift in Onset Potential of Solar Oxygen Evolution on Hematite by 13-group Oxide Overlayers. *Energy Environ. Sci.* **2011**, *4*, 2512−2515.
(19) Zhong, D. K.; Sun, J. W.; Inumaru, H.; Gamelin, D. R. Solar Water Oxidation by Composite Catalyst/α-Fe_2O_3 Photoanodes. *J. Am. Chem. Soc.* **2009**, *131*, 6086−6087.
(20) Du, C.; Yang, X.; Mayer, M. T.; Hoyt, H.; Xie, J.; McMahon, G.; Bischoping, G.; Wang, D. Hematite-based Water Splitting with Low Turn-On Voltages. *Angew. Chem., Int. Ed.* **2013**, *52*, 12692−12695.
(21) Liu, R.; Zheng, Z.; Spurgeon, J.; Yang, X. Enhanced Photoelectrochemical Water-Splitting Performance of Semiconductors by Surface Passivation Layers. *Energy Environ. Sci.* **2014**, *7*, 2504−2517.
(22) Yang, X.; Du, C.; Liu, R.; Xie, J.; Wang, D. Balancing Photovoltage Generation and Charge-Transfer Enhancement for Catalyst-decorated Photoelectrochemical Water Splitting: A Case Study of the Hematite/MnO_x Combination. *J. Catal.* **2013**, *304*, 86−91.
(23) Mor, G. K.; Prakasam, H. E.; Varghese, O. K.; Shankar, K.; Grimes, C. A. Vertically Oriented Ti-Fe-O Nanotube Array Films: Toward a Useful Material Architecture for Solar Spectrum Water Photoelectrolysis. *Nano Lett.* **2007**, *7*, 2356−2364.
(24) Cao, D.; Luo, W.; Feng, J.; Zhao, X.; Li, Z.; Zou, Z. Cathodic Shift of Onset Potential for Water Oxidation on a Ti^{4+} Doped Fe_2O_3 Photoanode by Suppressing the Back Reaction. *Energy Environ. Sci.* **2014**, *7*, 752−759.
(25) Franking, R.; Li, L. S.; Lukowski, M. A.; Meng, F.; Tan, Y. Z.; Hamers, R. J.; Jin, S. Facile Post-Growth Doping of Nanostructured Hematite Photoanodes for Enhanced Photoelectrochemical Water Oxidation. *Energy Environ. Sci.* **2013**, *6*, 500−512.
(26) Lin, Y.; Zhou, S.; Liu, X.; Sheehan, S.; Wang, D. TiO_2/$TiSi_2$ Heterostructures for High-Efficiency Photoelectrochemical H_2O Splitting. *J. Am. Chem. Soc.* **2009**, *131*, 2772−2773.
(27) Luber, E. J.; Buriak, J. M. Reporting Performance in Organic Photovoltaic Devices. *ACS Nano* **2013**, *7*, 4708−4714.
(28) Murphy, A. B.; Barnes, P. R. F.; Randeniya, L. K.; Plumb, I. C.; Grey, I. E.; Horne, M. D.; Glasscock, J. A. Efficiency of Solar Water Splitting Using Semiconductor Electrodes. *Int. J. Hydrogen Energy* **2006**, *31*, 1999−2017.
(29) Cherepy, N. J.; Liston, D. B.; Lovejoy, J. A.; Deng, H.; Zhang, J. Z. Ultrafast Studies of Photoexcited Electron Dynamics in γ- and α-Fe_2O_3 Semiconductor Nanoparticles. *J. Phys. Chem. B* **1998**, *102*, 770−776.
(30) Braun, A.; Sivula, K.; Bora, D. K.; Zhu, J.; Zhang, L.; Grätzel, M.; Guo, J.; Constable, E. C. Direct Observation of Two Electron Holes in a Hematite Photoanode during Photoelectrochemical Water Splitting. *J. Phys. Chem. C* **2012**, *116*, 16870−16875.
(31) Ong, J. L.; Lucas, L. C.; Raikar, G. N.; Gregory, J. C. Electrochemical Corrosion Analyses and Characterization of Surface-modified Titanium. *Appl. Surf. Sci.* **1993**, *72*, 7−13.
(32) Klahr, B.; Gimenez, S.; Fabregat-Santiago, F.; Bisquert, J.; Hamann, T. W. Photoelectrochemical and Impedance Spectroscopic Investigation of Water Oxidation with "Co-Pi"-Coated Hematite Electrodes. *J. Am. Chem. Soc.* **2012**, *134*, 16693−16700.
(33) Riha, S. C.; Klahr, B. M.; Tyo, E. C.; Seifert, S.; Vajda, S.; Pellin, M. J.; Hamann, T. W.; Martinson, A. B. F. Atomic Layer Deposition of a Submonolayer Catalyst for the Enhanced Photoelectrochemical Performance of Water Oxidation with Hematite. *ACS Nano* **2013**, *7*, 2396−2405.
(34) Bard, A. J.; Faulkner, L. R. *Electrochemical Methods: Fundamentals and Applications*, 2nd ed.; Wiley: New York, 2001; pp 92−107.
(35) Moir, J.; Soheilnia, N.; O'Brien, P.; Jelle, A.; Grozea, C. M.; Faulkner, D.; Helander, M. G.; Ozin, G. A. Enhanced Hematite Water Electrolysis Using a 3D Antimony-Doped Tin Oxide Electrode. *ACS Nano* **2013**, *7*, 4261−4274.
(36) Scheuermann, A. G.; Prange, J. D.; Gunji, M.; Chidsey, C. E. D.; McIntyre, P. C. Effects of Catalyst Material and Atomic Layer Deposited TiO_2 Oxide Thickness on the Water Oxidation Performance of Metal-Insulator-Silicon Anodes. *Energy Environ. Sci.* **2013**, *6*, 2487−2496.
(37) Gileadi, E. *Electrode Kinetics for Chemists, Chemical Engineers and Materials Scientists*; VCH Publishers, Inc.: New York, 1993.
(38) Guerrini, E.; Chen, H.; Trasatti, S. Oxygen Evolution on Aged IrO_x/Ti Electrodes in Alkaline Solutions. *J. Solid State Electrochem.* **2007**, *11*, 939−945.
(39) Fletcher, S. Tafel Slopes from First Principles. *J. Solid State Electrochem.* **2009**, *13*, 537−549.

(40) Bauer, H. H. The Electrochemical Transfer-Coefficient. *J. Electroanal. Chem. and Interface Electrochem.* **1968**, *16*, 419−432.
(41) Glasscock, J. A.; Barnes, P. R. F.; Plumb, I. C.; Savvides, N. Enhancement of Photoelectrochemical Hydrogen Production from Hematite Thin Films by the Introduction of Ti and Si. *J. Phys. Chem. C* **2007**, *111*, 16477−16488.
(42) Wang, G. M.; Ling, Y. C.; Wheeler, D. A.; George, K. E. N.; Horsley, K.; Heske, C.; Zhang, J. Z.; Li, Y. Facile Synthesis of Highly Photoactive α-Fe_2O_3-based Films for Water Oxidation. *Nano Lett.* **2011**, *11*, 3503−3509.
(43) Du, C.; Zhang, M.; Jang, J.-W.; Liu, Y.; Liu, G.-Y.; Wang, D. Observation and Alteration of Surface States of Hematite Photoelectrodes. *J. Phys. Chem. C* **2014**, *118*, 17054−17059.
(44) Zandi, O.; Hamann, T. W. Enhanced Water Splitting Efficiency Through Selective Surface State Removal. *J. Phys. Chem. Lett.* **2014**, *5*, 1522−1526.